

# Coprecipitation of metal ions into calcite: an estimation of partition coefficients based on field investigation

Zhongwei Wang<sup>1,2</sup> · Jiubin Chen<sup>1,3</sup> · Hongming Cai<sup>3</sup> · Wei Yuan<sup>3</sup> · Shengliu Yuan<sup>3</sup>

Received: 4 September 2020 / Revised: 26 October 2020 / Accepted: 12 November 2020 / Published online: 23 November 2020  
© Science Press and Institute of Geochemistry, CAS and Springer-Verlag GmbH Germany, part of Springer Nature 2020

**Abstract** Trace elements (and their isotopes) in carbonates are commonly used to reconstruct paleoenvironment and paleoclimate. Understanding the processes and mechanisms of element incorporation into carbonates is thus crucial for using such geochemical parameters as paleoclimate proxies. In contrast to laboratory-based experimental results, the partitioning of trace metals between solid and solution phases in natural carbonate precipitation systems has rarely been reported. In this study, we investigated the partition coefficients of metal ions between solid and solution in the channel of the natural Baishuitai travertine system, Yunnan, China. Our results show that the partition coefficients of  $\text{Li}^+$ ,  $\text{Na}^+$ ,  $\text{Mg}^{2+}$ ,  $\text{Sr}^{2+}$  and  $\text{Ba}^{2+}$  are  $< 1$ , that of  $\text{Ni}^{2+}$  is approximately 1, and those of  $\text{Co}^{2+}$ ,  $\text{Mn}^{2+}$ ,  $\text{Zn}^{2+}$  and  $\text{Cu}^{2+}$  are  $> 1$ , consistent with the results found in previous experimental studies. Although

the substitution for  $\text{Ca}^{2+}$  is likely the main uptake process of these metals into calcite, depending on their ionic radius and charge, trace elements may also be incorporated by adsorption or physical entrapment. Our study shows that unlike laboratory experiments performed under specific conditions, the partitioning of metals between two phases in the natural travertine system could be controlled by several, even multiple, environmental factors (e.g., carbonate deposition rate, temperature, and pH), which should be taken into account when using trace metals (and their isotopes) in carbonate archives as a paleoclimate proxy.

**Keywords** Metal ions · Coprecipitation · Calcite · Partition coefficients · Field investigation

## 1 Introduction

Trace elements in carbonates are widely used for investigating and reconstructing the past surface environment and climate. The process and mechanism of the incorporation of elements into carbonate are the factors restricting the use of such geochemical parameters as paleoclimate proxies. Carbonate minerals mainly consist of calcite, aragonite, and dolomite, with  $\text{Ca}^{2+}$  and  $\text{Mg}^{2+}$  as the major cations (Gaffey 1987). As the radius and electrovalence of the cation  $\text{Sr}^{2+}$  are similar to those of  $\text{Ca}^{2+}$ ,  $\text{Sr}^{2+}$  can replace  $\text{Ca}^{2+}$  in carbonates, leading to the enrichment of  $\text{Sr}^{2+}$  in carbonate minerals (Mucci and Mors, 1983). Consequently,  $\text{Ca}^{2+}$ ,  $\text{Mg}^{2+}$ , and  $\text{Sr}^{2+}$ , together with elemental ratios such as  $\text{Sr}^{2+}/\text{Ca}^{2+}$  and  $\text{Mg}^{2+}/\text{Ca}^{2+}$ , have received the most attention in the study of inorganic carbonate precipitation and related applications. In addition to containing these alkaline earth metals, carbonate minerals may contain a small amount of metal cations such as  $\text{Li}^+$ ,  $\text{Na}^+$ ,  $\text{Co}^{2+}$ ,

✉ Jiubin Chen  
jbchen@tju.edu.cn  
Zhongwei Wang  
wangzhongwei@mail.gyig.ac.cn  
Hongming Cai  
caihongming@tju.edu.cn  
Wei Yuan  
yuan\_wei@tju.edu.cn  
Shengliu Yuan  
yuanshl05@163.com

<sup>1</sup> State Key Laboratory of Environmental Geochemistry, Institute of Geochemistry, Chinese Academy of Sciences, Guiyang 550081, China  
<sup>2</sup> University of Chinese Academy of Sciences, Beijing 100049, China  
<sup>3</sup> School of Earth System Science, Institute of Surface-Earth System Science, Tianjin University, Tianjin 300072, China

$\text{Ni}^{2+}$ ,  $\text{Mn}^{2+}$ ,  $\text{Cu}^{2+}$ ,  $\text{Zn}^{2+}$  and  $\text{Ba}^{2+}$  (Curti 1999). These elements, together with  $\text{Ca}^{2+}$  and  $\text{Mg}^{2+}$ , have been used to trace surface environment evolution and dynamics (Chen et al. 2015; Gaillardet et al. 1999; Liu et al. 2019; White 2011). Moreover, the geochemical characteristics of various chemical components in carbonates have also been of great interest in the study of the geochemistry of sedimentary carbonate deposition and diagenesis (Roberts et al. 1998). In addition to the physicochemical characteristics of the elements themselves, external environmental parameters (such as temperature, pH, humidity, salinity, and precipitation rate) determine and control the incorporation of elements into carbonates. External environmental parameters could also restrict the element distribution coefficients between solid and solution phases (Füger et al. 2019).

The study of geochemical indexes related to this kind of mineral started with marine sedimentary carbonates (such as coral, benthic foraminifera, and zooplankton foraminifera) (Carpenter et al. 1991; Graham et al. 1982). Since then, a number of factors that were not previously considered to be important have been found to exert major influences on carbonate precipitation and related element partitioning. Laboratory experiments have been performed to investigate the impact of these factors on element behaviors during carbonate formation using both natural and synthetic seawater (Katz 1973; Kinsman and Holland 1969; Lorens 1981). It is generally believed that among other factors, seawater temperature and carbonate precipitation rate (depending on the degree of supersaturation of the solution) are the two most likely factors controlling the chemical composition of marine carbonate. Kinsman and Holland (1969) found that the partition coefficient of  $\text{Sr}^{2+}$  between calcite and aqueous solution decreased linearly with increasing temperature, from  $1.17 \pm 0.04$  at  $16^\circ\text{C}$  to  $0.88 \pm 0.03$  at  $80^\circ\text{C}$ , inconsistent with the results of Katz (1973), which showed only a slight influence. A later study showed that the partition coefficient of  $\text{Mg}^{2+}$  was closely related to temperature, the coefficients were  $0.0573 \pm 0.0017$  and  $0.1163 \pm 0.0034$  at  $25$  and  $80^\circ\text{C}$ , respectively (Katz 1973). Both studies found that the presence of other salts (such as  $\text{NaCl}$ ) did not affect the partition coefficients of  $\text{Sr}^{2+}$  and  $\text{Mg}^{2+}$ . In addition to temperature, the precipitation rate also impacts the distribution and geochemistry of elements during carbonate precipitation. Lorens (1981) showed that the partition coefficient of  $\text{Sr}^{2+}$  increases with an increasing calcite deposition rate. Mucci and Morse (1983) measured the contents of  $\text{Mg}^{2+}$  and  $\text{Sr}^{2+}$  in calcite precipitated in both natural and synthetic seawater at  $25^\circ\text{C}$  and found that the partition coefficients of  $\text{Mg}^{2+}$  and  $\text{Sr}^{2+}$  did not change significantly when the deposition rate changed by an order of magnitude. The same result was observed by Mucci (1987). Recently, Mavromatis et al. (2013) showed that the

partition coefficient of  $\text{Mg}^{2+}$  was positively related to the deposition rate of calcite. In addition to temperature and deposition rate, other factors, such as the partial pressure of carbon dioxide in solution, may also impact the content of  $\text{Mg}^{2+}$  in carbonates (Burton and Walter 1991).

Apart from  $\text{Mg}^{2+}$  and  $\text{Sr}^{2+}$ , other metal ions such as  $\text{Li}^+$ ,  $\text{Na}^+$ ,  $\text{Co}^{2+}$ ,  $\text{Ni}^{2+}$ ,  $\text{Mn}^{2+}$ ,  $\text{Zn}^{2+}$ ,  $\text{Cu}^{2+}$ ,  $\text{Cr}^{2+}$ , and  $\text{Ba}^{2+}$  have also been studied in inorganic carbonate deposition experiments to test the usefulness of these parameters as environmental proxies. The results showed that the partition coefficients of  $\text{Co}^{2+}$ ,  $\text{Mn}^{2+}$ , and  $\text{Cd}^{2+}$  decreased with an increased deposition rate of calcite (Lakshatanov and Stipp 2007; Lorens 1981) while those of  $\text{Li}^+$  and  $\text{Na}^+$  increased with increasing deposition rate (Füger et al. 2019). In addition, White (1977) found that the partition coefficient of  $\text{Na}^+$  was related to the  $\text{Ca}^{2+}$  activity and pH of the reaction solution.

In addition to the geochemistry of a single element, elemental ratios or couplings such as  $\text{Sr}^{2+}/\text{Ca}^{2+}$ ,  $\text{Mg}^{2+}/\text{Ca}^{2+}$ ,  $\text{Cd}^{2+}/\text{Ca}^{2+}$ ,  $\text{Sr}^{2+}/\text{Ba}^{2+}$ , and  $\text{Zn}^{2+}/\text{Ba}^{2+}$  have been widely used for reconstructing past environmental changes, such as temperature and salinity variations (Carpenter et al. 1991; Graham et al. 1982; Rosenthal et al. 1997). For example, the changes in the ion ratios  $\text{Mg}^{2+}/\text{Ca}^{2+}$  and  $\text{Sr}^{2+}/\text{Ca}^{2+}$  in secondary sedimentary carbonate (stalagmite) are influenced by various climatic and environmental factors on a local or regional scale (Gascoyne 1983; Luo et al. 2013; Roberts et al. 1998). Roberts et al. (1998) found that the annual  $\text{Mg}^{2+}/\text{Ca}^{2+}$  oscillations may be caused by seasonal temperature changes, while the influence of external humidity would be more important for long-time-scale research. In Belgium and southern Brazil,  $\text{Mg}^{2+}/\text{Ca}^{2+}$  and  $\text{Sr}^{2+}/\text{Ca}^{2+}$  in stalagmites were suggested to be mostly controlled by changes in precipitation (Roberts and Wright 1993).

Although these previous studies have substantially improved our knowledge of the distribution and geochemistry of alkaline earth elements during the formation of carbonates, they have sometimes reported inconsistent or even contrasting results. In addition, the geochemical behaviors of other elements, such as  $\text{Li}^+$ ,  $\text{Na}^+$ ,  $\text{Co}^{2+}$ ,  $\text{Ni}^{2+}$ ,  $\text{Mn}^{2+}$ ,  $\text{Cu}^{2+}$ , and  $\text{Zn}^{2+}$ , with respect to carbonate precipitation processes remain unclear. Moreover, most of this knowledge was obtained from laboratory experiments, and large uncertainties would exist when applying these results to the reconstruction of the paleoenvironment. Therefore, in order to better understand the incorporation of elements into solids and its related mechanisms, more systematic studies should be performed on the geochemistry of trace elements in natural carbonate archives, such as travertine. This would be useful for the precise application of these parameters in investigating and reconstructing the past surface environment. In this paper, we investigated the

distribution of some typical metal elements ( $\text{Li}^+$ ,  $\text{Na}^+$ ,  $\text{Co}^{2+}$ ,  $\text{Ni}^{2+}$ ,  $\text{Mg}^{2+}$ ,  $\text{Ca}^{2+}$ ,  $\text{Mn}^{2+}$ ,  $\text{Cu}^{2+}$ ,  $\text{Zn}^{2+}$ ,  $\text{Sr}^{2+}$ , and  $\text{Ba}^{2+}$ ) during surface carbonate precipitation in the natural Baishuitai travertine system, Yunnan, China. The objectives of this work are (1) to investigate the geochemistry of metal elements during travertine formation, (2) to assess the partition coefficients of different metal ions between the solid and liquid phases, and (3) to identify the factors impacting the partition coefficients of metal ions in the natural travertine system.

## 2 Methods

### 2.1 Sampling site

The Baishuitai travertine site ( $27^{\circ}30' \text{ N}$ ,  $100^{\circ}02' \text{ E}$ ) is located approximately 103 km south of Shangri-La Town, Yunnan Province, China (Fig. 1), with an average elevation of approximately 2380 m above sea level. The area is characterized by a subtropical monsoon climate, with  $> 75\%$  ( $\sim 750 \text{ mm}$ ) of the annual precipitation occurring during the rainy season from May to October. The annual mean air temperature is approximately  $8^{\circ}\text{C}$  (Liu et al. 2003). The area features a typical karst landscape and hosts one of the largest travertine deposits in China, the Baishuitai travertine system. The travertine forms during calcite precipitation from supersaturated groundwater.

The endogenic travertine samples in this study were collected along a 2.6 km-long canal. The water in the canal was supplied mainly by a spring, with limited water contribution from the adjacent Baishuitai River. When spring

water emerged, a vast quantity of  $\text{CO}_2$  was released to the atmosphere, creating an increase in the saturation state of calcite and thus leading to simultaneous calcite precipitation from the water (Yan et al. 2016).

### 2.2 Sample collection and preparation

In December 2013, a set of surface water and travertine samples were simultaneously collected along the canal (Fig. 1). To obtain the in situ formed travertine samples, plexiglass substrate plates ( $15 \times 15 \text{ cm}$ ) were placed in the water (8 cm deep, in the middle of the canal) at 11 different sites (numbered 1–11) along the canal. Water samples were collected in 2 L precleaned polypropylene containers (Nalgene, America) and then filtered through  $0.45 \mu\text{m}$  Millipore express membrane filters immediately after collection. Solutions for cation concentration measurements were acidified to  $\text{pH} < 2$  with double-distilled  $\text{HNO}_3$ . An aliquot of the solution was not acidified and was prepared for major anion concentration analysis. The precipitated solid travertine samples on the plexiglass plates were transported to the laboratory in 50 mL polypropylene tubes, freeze-dried, and crushed in a mortar for further treatment.

To measure the trace metal concentration contained only in pure carbonates and avoid the dissolution of other substances, approximately 0.5 g of powdered travertine was dissolved in 20 mL 6% acetic acid (v/v) for approximately 24 h to ensure sufficient time and acid to completely dissolve calcium carbonate (Liu et al. 2013). The samples were then centrifuged, and the supernatants were collected with pipettes and transferred to Teflon beakers. After



**Fig. 1** Location of samples in the Baishuitai travertine canal system, Yunnan Province, China

evaporation at 100 °C, the residue was dissolved again in 3% HNO<sub>3</sub> for concentration measurements via inductively coupled plasma-mass spectrometry (ICP-MS).

### 2.3 Chemical parameter analysis

The in situ temperature, pH, dissolved oxygen content, and conductivity of water at each sampling site in the canal were measured using a hand-held multiparameter analyzer (WTW 3430, WTW, Germany), with resolutions of 0.2 °C, 0.004, 0.01 mg/L and 1 μS/cm (micro-Siemens/cm), respectively. The concentrations of Na<sup>+</sup>, Sr<sup>2+</sup>, Mg<sup>2+</sup>, and Ca<sup>2+</sup> were measured with an inductively coupled plasma optical emission spectrometer (ICP-OES) with a precision generally better than 10%. Selected trace elements were analyzed on a Perkin-Elmer Elan 6000 quadrupole ICP-MS with the addition of an indium solution as an internal standard. The precision of trace element measurements was generally better than 5%. Typical travertine samples were selected for mineral phase analysis by X-ray diffraction (XRD). Scanning electron microscopy (SEM) measurements were also performed to characterize the calcite crystal shapes and habits. All measurements were made at the State Key Laboratory of Environmental Geochemistry of the Institute of Geochemistry, Chinese Academy of Sciences, Guiyang, China.

### 2.4 Carbonate deposition rate calculation

In this study, the carbonate deposition rate ( $R$ ), expressed in mol m<sup>-2</sup> s<sup>-1</sup>, was approximately estimated as the amount of travertine deposited in a given time period on the plexiglass plates by subtracting the weight of the plate:

$$R = (W - W_0)/(S \times T) \quad (1)$$

where  $W$  and  $W_0$  are the weights of the plexiglass substrates after and before each experimental run, respectively.  $T$  is the sample collection duration for each run (30 days), and  $S$  is the surface area for precipitation, which was roughly estimated as the total surface area of the substrate (225 cm<sup>2</sup>).

### 2.5 Metal ion partitioning between calcite and solution

The definition of the apparent partition coefficient  $K_{me}$  is adopted in this paper, which is applied to coprecipitation with calcite, conforming to what is given in the paper of Doerner and Hoskins (1925):

$$K_{Me} = ([Me]/[Ca])_{\text{calcite}} / ([Me]/[Ca])_{\text{aq}} \quad (2)$$

where  $([Me]/[Ca])_{\text{calcite}}$  is the  $Me/Ca$  molar ratio of precipitated calcite and  $([Me]/[Ca])_{\text{aq}}$  is the  $Me/Ca$  molar ratio of the solution.

## 3 Result

### 3.1 Geochemical characteristics of water samples

The geochemical parameters of the 11 water samples are listed in Table 1. The speciation, CaCO<sub>3</sub> saturation index ( $SI_{\text{CaCO}_3}$ ) with respect to calcite, CO<sub>2</sub> partial pressure ( $P_{\text{CO}_2}$ ), and ionic strength ( $I$ ) of the solution is calculated using PHREEQC software with its Visual MINTEQ V4 database and are also listed in Table 1. From sites 1 to 11 (with the direction of water flow from upstream to downstream), the pH display a relatively small change between 7.98 and 8.21, but the water temperature gradually decrease from 6.2 to 1.5 °C, the salinity increase from 0.62 to 0.4, and  $P_{\text{CO}_2}$  drop from 349 to 189 Pa. According to the speciation calculation results, Ca<sup>2+</sup> and HCO<sub>3</sub><sup>-</sup> free ions account for more than 99% of the total ions present in the solution. The logarithmic variation in the deposition rate ranges from - 6.00 to - 5.09. The results also show that the reactions all occur at a relatively constant ionic strength ( $I = 0.01$  mol kg<sup>-1</sup>).  $SI_{\text{CaCO}_3}$  is greater than 0, indicating that calcium carbonate is in a supersaturated state at all sample sites.

### 3.2 Mineralogy and geochemical composition of the precipitate

The XRD patterns of all solid samples analyzed in this study indicate that calcite is the main phase precipitated in the water flow course (the detection limit of XRD analysis was 2 wt%), which is consistent with previous studies (Liu et al. 2006; Yan et al. 2016). In accordance with the XRD results, SEM images show that the precipitated solids maintained the rhombic morphology of calcite with overgrowth features on the solid surface (Fig. 2).

### 3.3 Metal ion partitioning between calcite and solution

In Table 1, we list the calculated partition coefficients for elements that have been investigated in previous studies (Crocket and Winchester 1966; Curti 1999; Doerner and Hoskins 1925; Elzinga et al. 2006; Füger et al. 2019; Gascoyne 1983; Lorens 1981; Mavromatis et al. 2013; Mucci and Morse 1983; Okumura and Kitano 1986; Pingitore and Eastman 1984, 1986; Reeder et al. 1999; Rimstidt et al. 1998; Tesoriero and Pankow 1996). The

**Table 1** General hydrochemical composition of the Baishuitai canal

Site	Distance to spring (km)	$\log R$ (mol m <sup>-2</sup> s <sup>-1</sup> )	pH	$I$ (mol kg <sup>-1</sup> )	Salinity (psu)	$T$ (°C)	$SI_{CaCO_3}$	$P_{CO_2}$ (pa)	$K_{Li}^+$	$K_{Na}^+$	$K_{Mg}^{2+}$	$K_{Mn}^{2+}$	$K_{Co}^{2+}$	$K_{Ni}^{2+}$	$K_{Cu}^{2+}$	$K_{Zn}^{2+}$	$K_{Sr}^{2+}$	$K_{Ba}^{2+}$
1	0.2	-5.14	7.98	0.014	0.62	6.2	1.08	349	0.007	0.003	0.007	3.357	2.412	1.012	2.598	15.018	0.217	0.425
2	0.3	-5.12	8.12	0.014	0.60	5.9	1.23	244	0.003	0.003	0.009	2.998	2.734	1.127	3.069	19.803	0.225	0.485
3	0.7	-5.12	8.21	0.012	0.58	5.5	1.21	188	0.006	0.003	0.008	3.644	2.140	0.830	2.079	22.614	0.197	0.358
4	0.8	-5.20	8.14	0.013	0.57	5.4	1.18	213	0.003	0.003	0.009	1.699	1.790	0.992	1.570	8.346	0.209	0.391
5	1.1	-5.09	8.18	0.012	0.52	6.1	1.14	187	0.005	0.002	0.007	0.219	0.289	0.595	2.952	6.122	0.193	0.423
6	1.4	-5.24	8.20	0.009	0.50	5.1	0.98	172	0.005	0.002	0.005	0.351	0.804	0.716	3.124	8.840	0.136	0.288
7	1.8	-5.38	8.18	0.010	0.48	4.2	0.98	166	0.007	0.002	0.007	4.989	1.398	0.836	1.307	4.306	0.165	0.353
8	2.0	-5.46	8.16	0.010	0.48	3.6	0.97	176	0.005	0.002	0.008	2.760	1.917	0.922	1.334	7.886	0.175	0.365
9	2.4	-6.00	8.05	0.009	0.46	2.4	0.78	218	0.005	0.003	0.009	4.205	1.409	0.728	1.306	8.078	0.131	0.255
10	2.5	-5.83	8.13	0.009	0.46	2.2	0.83	180	0.007	0.003	0.008	2.185	1.637	0.914	0.832	9.502	0.140	0.270
11	2.6	-5.67	8.09	0.009	0.40	1.5	0.78	189	0.004	0.002	0.008	5.799	1.992	0.860	10.220	2.749	0.174	0.339

partition coefficients are relatively smaller for  $Li^+$ ,  $Na^+$ ,  $Mg^{2+}$ ,  $Sr^{2+}$ , and  $Ba^{2+}$ , varying from 0.003 to 0.007, from 0.002 to 0.003, from 0.005 to 0.009, from 0.131 to 0.225 and from 0.255 to 0.485 respectively. However, those for  $Mn^{2+}$  (from 0.219 to 5.799),  $Co^{2+}$  (from 0.289 to 2.734),  $Ni^{2+}$  (from 0.595 to 1.127),  $Cu^{2+}$  (from 0.832 to 10.220) and  $Zn^{2+}$  (from 2.749 to 22.614) are bigger and show large variation. The partition coefficients of the ions  $Li^+$ ,  $Na^+$ ,  $Mg^{2+}$ ,  $Sr^{2+}$ , and  $Ba^{2+}$  are inferior to 1, the partition coefficient of  $Ni^{2+}$  is approximately 1, and the partition coefficients of  $Co^{2+}$ ,  $Mn^{2+}$ ,  $Zn^{2+}$ , and  $Cu^{2+}$  are higher than 1. Notably, these values for the natural travertine system are generally in agreement with those for experimental simulations, as summarized in Table 2 (Crocket and Winchester 1966; Dromgoole and Walter 1990; Katz 1973; Kitano et al. 1980; Lorens 1981; Mucci and Morse 1983; Pingitore and Eastman 1986; Tesoriero and Pankow 1996; Zhong and Mucci 1995). More precisely, the partition coefficients of  $Li^+$ ,  $Na^+$ ,  $Co^{2+}$ ,  $Ni^{2+}$ ,  $Mg^{2+}$ ,  $Zn^{2+}$ , and  $Sr^{2+}$  are in the same range as or largely overlapped with published experimental data; the partition coefficients of  $Mn^{2+}$  and  $Cu^{2+}$  are slightly lower than laboratory simulation results; the partition coefficient of  $Ba^{2+}$  is higher than that of the laboratory simulation but consistent with the field observations by Drake et al. (2017).

## 4 Discussion

### 4.1 Occurrence or absence of thermodynamic equilibrium

We first evaluated whether the travertine precipitation is equilibrium. Establishing equilibrium conditions is the key point for assessing the distribution characteristics of elements between water and carbonate. The calcites are precipitated from oversaturated water with a relatively high flowrate (approximately 1 ms<sup>-1</sup>), which would not allow for a complete exchange of metal ions between solution and solid phases, suggesting that an equilibrium state was unlikely. This conclusion could be further confirmed by the fact that only a small proportion of aqueous metal ions are precipitated or incorporated into the solid phase during travertine formation (e.g., < 0.03% for  $Mg^{2+}$  and < 8% for  $Zn^{2+}$ ). Moreover, according to the thermodynamic model, at 298 K and 1 bar, a linear relationship should exist between  $\ln K_{Me}$  (the natural logarithm of the partition coefficient) and the free energy difference ( $\Delta G_{Ca}^0 - \Delta G_{Me}^0$ ) for equilibrium precipitation (Sverjensky 1984). Assuming that the reaction between  $Me$  in solution and  $Ca^{2+}$  in the solid phase reaches chemical equilibrium, we should be able to predict the linear correlation between the partition coefficient of  $Me$  in the carbonate-solution

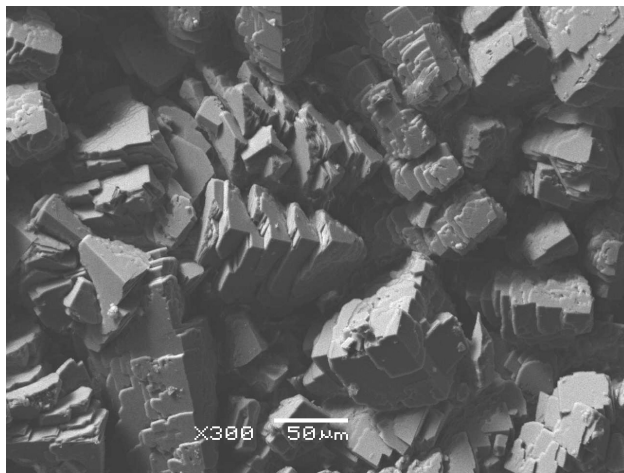


**Fig. 2** Scanning electron microphotographs of final overgrown precipitates showing a mainly calcite crystal structure

system and the difference in the standard Gibbs free energies of Me and  $\text{Ca}^{2+}$ . As shown in Fig. 3,  $\ln K_{\text{Me}}$  versus the free energy difference between  $\text{Ca}^{2+}$  and other ions (Me) displays no obvious correlation (Fig. 3).

Previous experimental studies of carbonate precipitation in the laboratory show that equilibrium between the solution and the precipitated carbonate is difficult for metal ions to attain even at a long time scale (i.e., with a much slower precipitation rate) (Morse and Bender 1990; Sverjensky 1984). We hypothesize that no equilibrium state is attained in our travertine precipitation system. Figure 3 demonstrates that ions such as  $\text{Sr}^{2+}$ ,  $\text{Ba}^{2+}$ , and  $\text{Mg}^{2+}$ , which possess free energies similar to that of  $\text{Ca}^{2+}$ , have a partition coefficient  $K_{\text{Me}} < 1$ , whereas ions such as  $\text{Cu}^{2+}$ ,  $\text{Mn}^{2+}$  and  $\text{Ni}^{2+}$  with free energies drastically different from that of  $\text{Ca}^{2+}$ , had  $K_{\text{Me}} > 1$ . This trend is similar to the features of metal partitioning observed in carbonate precipitation systems in laboratory experiments (Sverjensky 1984). However, the relationship between the partition coefficient and the free energy difference is not consistent with the prediction of equilibrium (Fig. 3). Therefore, the equilibrium exchange of metal ions between solution and carbonates would rarely be attained for either laboratory simulations or natural systems.

As a result, the geochemical behaviors and element partitioning could not be predicted and simply explained by the thermodynamic model. Practically, the understanding of partition coefficients is complicated by the fact that true thermodynamic equilibrium is rarely if ever, obtained under near-Earth-surface conditions. Partition coefficients are not equivalent to thermodynamic constants, generally represent phenomenological measurements under certainly given sets of conditions, and are influenced by other factors, including both internal ion physicochemical characteristics and external environmental parameters.

**Table 2** Compilation of literature data on the coprecipitation of metals in calcite

Cation	Partition coefficient range	This study
$\text{Li}^{+}$	$10^{-5.1}$ –0.009 <sup>a</sup>	0.003–0.007
$\text{Na}^{+}$	$10^{-5.1}$ –0.006 <sup>b</sup>	0.002–0.003
$\text{Mg}^{2+}$	0.010–0.124 <sup>c</sup>	0.005–0.009
$\text{Mn}^{2+}$	3.1–33.3 <sup>d</sup>	0.219–5.799
$\text{Co}^{2+}$	1.9–5.9 <sup>e</sup>	0.289–2.734
$\text{Ni}^{2+}$	0.94–1.12 <sup>f</sup>	0.595–1.127
$\text{Cu}^{2+}$	23.3–25 <sup>g</sup>	0.832–10.220
$\text{Zn}^{2+}$	1.6–80 <sup>h</sup>	2.749–22.614
$\text{Sr}^{2+}$	0.02–0.40 <sup>i</sup>	0.131–0.225
$\text{Ba}^{2+}$	0.003–0.12 <sup>j</sup>	0.255–0.485

<sup>a</sup>Data from Okumura and Kitano (1986), Föger et al. (2019)

<sup>b</sup>Data from Okumura and Kitano (1986), Zhong and Mucci (1995), Föger et al (2019)

<sup>c</sup>Data from Katz et al. (1972), Mucci and Morse (1983),

<sup>d</sup>Data from Lorens (1981), Dromgoole and Walter (1990)

<sup>e</sup>Data from Lorens (1981)

<sup>f</sup>Data from Lakshatanov and Stipp (2007)

<sup>g</sup>Data from Rimstidt et al. (1998)

<sup>h</sup>Data from Crocket and Winchester (1966), Kitano et al. (1980), Lorens (1981)

<sup>i</sup>Data from Katz (1973), Lorens (1981), Mucci and Morse (1983), Pingitore and Eastman (1986), Tesoriero and Pankow (1996)

<sup>j</sup>Data from Pingitore and Eastman (1984), Tesoriero and Pankow (1996)

## 4.2 Incorporation of metal ions into calcite

To better define paleoenvironment evaluations using geochemical proxies in surface carbonate archives, the most important consideration is the incorporation mechanism of metal ions into carbonates (Reeder et al. 1999). The mechanism is controlled by both the internal physicochemical characteristics of these ions and external environmental factors.

It is thought that metal ions can exist in carbonate minerals in various ways, including adsorption, coprecipitation, precipitation, and mechanical entrapment (Gaskova et al. 2009). Several studies have shown that in addition to the substitution of  $\text{Ca}^{2+}$  ions in the crystal lattice, other incorporation mechanisms (e.g., mechanical entrapment, the physical process of occlusion of adsorbates) may be operative in the sequestration of divalent trace metals by calcite, depending on reaction variables such as metal type and concentration, calcite saturation state, reaction time, and pH (Elzinga et al. 2006). During incorporation into carbonate crystal lattices, metal ions could eventually be adsorbed on the solid surface. Taking into account the

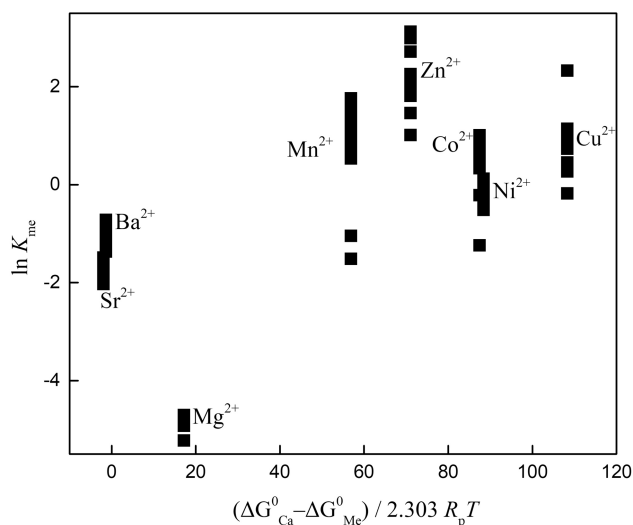


**Fig. 3** Calculated partition coefficients  $K_{me}$  for certain metal cations between calcite and aqueous solution as a function of the free energy difference between  $\text{Ca}^{2+}$  and the metal ion  $\text{Me}^{2+}$  (where  $\text{Me}^{2+}$  is  $\text{Co}^{2+}$ ,  $\text{Ni}^{2+}$ ,  $\text{Mg}^{2+}$ ,  $\text{Mn}^{2+}$ ,  $\text{Cu}^{2+}$ ,  $\text{Zn}^{2+}$ ,  $\text{Sr}^{2+}$  and  $\text{Ba}^{2+}$ ).  $R_p = 0.008306 \text{ kJ/K}\cdot\text{mol}$ ,  $T = 298 \text{ K}$

rapid deposition of calcite from water, a certain proportion of metal ions would also be taken up into calcite through mechanical entrapment (Elzinga et al. 2006). However, considering the relatively small free spaces in the solid phase, this proportion of metal ions (absorbed in or occupying the spaces) would likely be very limited. Although we could not identify the exact speciation of metals in the calcites at this stage, the substitution of cations ( $\text{Ca}^{2+}$ ) could be the dominant incorporation mechanism. Spectroscopic techniques have provided direct confirmation that metal ions with sizes either significantly smaller or larger than that of host  $\text{Ca}^{2+}$  can substitute  $\text{Ca}^{2+}$  in the calcite structure with varying amounts of local distortion (Elzinga et al. 2006). In fact, the sizes and charges of coprecipitates are the most important parameters in predicting the partitioning of elements between the two phases (dissolved and solid) and the relative impacts of chemical parameters (Curti 1999). Ions with a radius similar to that of the replaced ion ( $\text{Ca}^{2+}$ ) and the same charge would be more effectively bound in the lattice than would ions with different sizes and charges. Thus, cations with a sharp difference in radius from that of  $\text{Ca}^{2+}$  would usually have a lower content (and thus a smaller partition coefficient) in carbonate because they are either too large or too small to occupy the octahedral lattice as  $\text{Ca}^{2+}$  does in calcite (Curti 1999).

Table 3 summarizes the effective ionic radii of the ions  $\text{Li}^+$ ,  $\text{Na}^+$ ,  $\text{Co}^{2+}$ ,  $\text{Ni}^{2+}$ ,  $\text{Mg}^{2+}$ ,  $\text{Ca}^{2+}$ ,  $\text{Mn}^{2+}$ ,  $\text{Cu}^{2+}$ ,  $\text{Zn}^{2+}$ ,  $\text{Sr}^{2+}$  and  $\text{Ba}^{2+}$  in six-fold coordination. In Fig. 4, the relationship between the partition coefficients and the ionic radii of the coprecipitation ions does not show a good

correlation as a whole. However, the ions with  $K_{Me} > 1$  whose ionic radius is smaller than that of  $\text{Ca}^{2+}$  had a positive correlation between the partition coefficient and ionic radius. This correlation is consistent with the predicted behavior; that is, the closer the radius of the ion is to that of the substituted ion  $\text{Ca}^{2+}$ , the more easily it can replace  $\text{Ca}^{2+}$  in carbonate, generally resulting in a greater partition coefficient. However, this trend does not apply for ions with a  $K_{Me}$  less than 1. It is interesting to note that although  $\text{Zn}^{2+}$  ( $K_{Me} > 1$ ) and  $\text{Mg}^{2+}$  ( $K_{Me} < 1$ ) possess the same charge and similar ionic radius, they have different partition coefficients. In fact, the high hydration energy and a strong affinity with  $\text{H}_2\text{O}$  molecules in an aqueous solution of Mg likely contribute to the peculiar behavior of this element (Mavromatis et al. 2013). Furthermore, transition metals such as  $\text{Cu}^{2+}$ ,  $\text{Zn}^{2+}$ , and  $\text{Ni}^{2+}$  ( $K_{Me} > 1$ ) have unique electrons in the d-orbitals, leading to a much lower ligand stabilization energy (LSE). Thus, these transition metals more readily form stronger complexes with oxygen donor ligands than do alkaline earth metals such as  $\text{Sr}^{2+}$ ,  $\text{Ba}^{2+}$ , and  $\text{Mg}^{2+}$  ( $K_{Me} < 1$ ) (Schott et al. 2014; White 2011). This property may be one of the reasons for the difference in partition coefficients between transitional elements and alkali metal elements in calcium carbonate. However, whether the partitioning of these metals between water and calcite is in equilibrium and the related controlling factors need to be further systematically investigated through both field and laboratory studies.

Therefore, the incorporation of  $\text{Me}^+$  ions into the calcite lattice is primarily controlled by their ionic radii and charge. Other environmental factors (e.g., temperature) may also impact the distribution of metal ions during travertine precipitation, especially for ions with  $K_{me} < 1$ .

#### 4.3 Partitioning of metals between water and carbonate

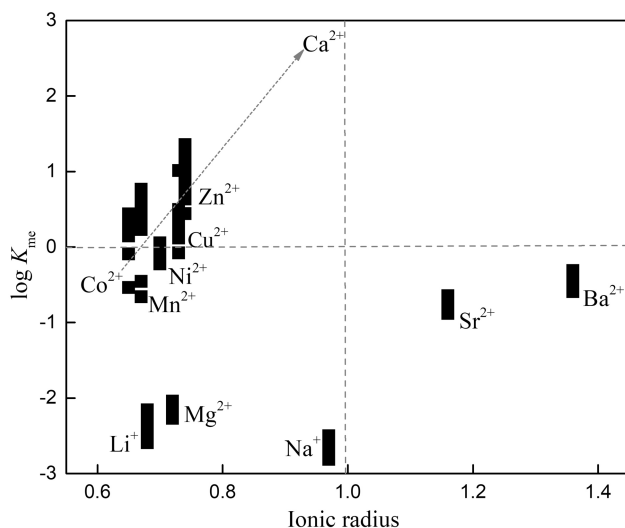
The partition coefficient is a key parameter for describing the partitioning of metal ions between water and solid in the travertine system. This parameter is controlled by element physicochemical characteristics and external environmental parameters. In the following, we investigate the effects of parameters such as the temperature, carbonate deposition rate, and pH on the partition coefficients of ions in our travertine system.

##### 4.3.1 Possible effects of temperature and pH

Some previous experimental studies show that the partition coefficients of metal ions might be affected by geochemical parameters such as the temperature and pH of water solutions under a given set of conditions. Föger et al. (2019) reported that the partition coefficients of  $\text{Li}^+$  and  $\text{Na}^+$  in

**Table 3** Effective ionic radii in six-fold coordination and standard free energies (at 298 K and 1 bar) for ions considered in this paper

Cation	$r(\text{VI}) (\text{\AA})^a$	$\Delta G_{298}^0 (\text{kcal/mole})^b$
$\text{Li}^+$	0.68	
$\text{Na}^+$	0.97	
$\text{Mg}^{2+}$	0.72	− 108.70
$\text{Ca}^{2+}$	0.99	− 132.20
$\text{Mn}^{2+}$	0.67	− 54.50
$\text{Co}^{2+}$	0.65	− 12.80
$\text{Ni}^{2+}$	0.70	− 11.53
$\text{Cu}^{2+}$	0.73	15.65
$\text{Zn}^{2+}$	0.74	− 35.20
$\text{Sr}^{2+}$	1.16	− 134.77
$\text{Ba}^{2+}$	1.36	− 134.02

<sup>a</sup>Data from Shannon and Prewitt (1969)<sup>b</sup>Data from Gaskova et al. (2009)**Fig. 4** Graphical representation of the partition coefficients of selected metal cations between calcite and solution as a function of the ionic radius of the coprecipitated ion

carbonate are related to the activity of  $\text{Ca}^{2+}$  ions in the reaction solution and the pH. For example,  $K_{\text{Li}}$  exhibits a strong decrease from  $10^{-3.3}$  to  $10^{-5.1}$  as the pH increase from 6.3 to 9.5. The distribution coefficient of Mg shows a positive correlation with temperature, with values of  $0.0121 \pm 0.0013$  at 5 °C,  $0.0172 \pm 0.0022$  at 25 °C, and  $0.0271 \pm 0.0013$  at 40 °C (Mucci and Morse 1983). However, the partition coefficient of  $\text{Zn}^{2+}$  in carbonate deposition is negatively related to the temperature (and salinity) of the solution (Tsusue and Holland 1966). Notably, these results are mainly obtained from laboratory experiments with a relatively large variation range in

geochemical parameters, and the effects of small variations in temperature and pH in a natural system remain unclear. In this study, we do not observe any correlations between these two parameters with the partition coefficients of the metals  $\text{K}^+$ ,  $\text{Na}^+$ ,  $\text{Mg}^{2+}$ , and  $\text{Zn}^{2+}$ . In fact, the pH of the water solution in our travertine system is quasi-constant (between 7.98 and 8.21), and the temperature also displays only a small variation range (gradually decreasing from 6.2 to 1.5 °C). This relative consistency may be one of the reasons why the effects of temperature and pH on metal distribution would likely be limited.

#### 4.3.2 Effect of calcite deposition rate

Figure 5 indicates the partition coefficients as a function of the deposition rate of calcium carbonate. It should be noted that we were not able to exactly measure the seed crystal surface area at this stage for a given degree of solution saturation; the deposition rate calculated by Eq. 1 is not the true calcium carbonate precipitation rate. We could assume a close proportional relationship between the deposition rate calculated by Eq. 1 and the true precipitation rate.

The overall logarithmic variation in the deposition rate ranges from − 6.00 to − 5.09, and the deposition rate exhibits a linear correlation with the  $\text{SI}_{\text{CaCO}_3}$  saturation degree of the solution with respect to calcite. For ions with  $K_{\text{Me}} < 1$ , the partition coefficients of  $\text{Sr}^{2+}$  and  $\text{Ba}^{2+}$  increase with increasing calcium carbonate deposition rate, but correlations for  $\text{Li}^+$ ,  $\text{Na}^+$ , and  $\text{Mg}^{2+}$  are not obvious. In addition, for ions with  $K_{\text{Me}} > 1$ , there is no similar relationship, except that the partition coefficient of  $\text{Mn}^{2+}$  decreases with increasing calcium carbonate deposition rate.

The effects of growth rate during calcium carbonate mineral precipitation have been documented for a large number of traces/impurities. Lorens (1981) indicated that the partition coefficient of  $\text{Sr}^{2+}$  increased with the calcite deposition rate, while those of  $\text{Co}^{2+}$ ,  $\text{Mn}^{2+}$ , and  $\text{Cd}^{2+}$  decreased. Mavromatis et al. (2013) and Füger et al. (2019) observed that the partition coefficients of  $\text{Mg}^{2+}$ ,  $\text{Li}^+$ , and  $\text{Na}^+$  increased with increasing calcite deposition rate. However, Mucci and Morse (1983) measured the contents of  $\text{Mg}^{2+}$  and  $\text{Sr}^{2+}$  during calcite precipitation from natural and synthetic seawater at 25 °C and found that when the deposition rate of calcite changed by an order of magnitude, the contents of  $\text{Mg}^{2+}$  and  $\text{Sr}^{2+}$  did not vary significantly, indicating that there was no significant effect of this parameter on the distribution of  $\text{Mg}^{2+}$  and  $\text{Sr}^{2+}$ . Therefore, the precipitation rate has displayed controversial effects on the partition coefficients of metal ions in surface carbonate systems (Morse and Bender 1990). In fact, kinetic influences could cause both increases and decreases in the partition coefficients of metal elements between solid and

solution phases. At high precipitation rates, there is even a chance for the physical process of occlusion of adsorbates to occur. However, as described by Rimstidt et al. (1998), with increasing growth rate, elemental partitioning during incorporation into a carbonate mineral phase tends towards unity. Consequently, this behavior implies that the partition coefficients of ions with  $K_{Me} < 1$  (such as  $Ba^{2+}$ ,  $Sr^{2+}$ ,  $Li^+$  and  $Na^+$ ) increase with the calcite deposition rate, while the partition coefficients of ions with  $K_{Me} > 1$  (such as  $Co^{2+}$ ,  $Mn^{2+}$  and  $Cd^{2+}$ ) decrease with the calcite deposition rate. Because the partition coefficient of  $Ni^{2+}$  is approximately 1, the change in the  $Ni^{2+}$  partition coefficient with the deposition rate of calcite is not obvious.

The impact of deposition rate on metal ion partitioning between calcite and water could be explained by the growth entrapment model (GEM) developed by Watson and coworkers (Füger et al. 2019; Mavromatis et al. 2013; Watson 1996, 2004). Over the last decades, GEM has been successfully applied to many cases to describe elemental cation partitioning between carbonate minerals and fluids. According to the model, a trace element incorporated in a growing crystal could be either enriched or depleted in the near-surface layer because this region is structurally distinct from the bulk lattice. Cations such as  $Ba^{2+}$  or  $Sr^{2+}$ , which are relatively incompatible in the calcite lattice ( $K_{Me} < 1$ ), would be enriched in the distorted and hydrated thin layer (< 1 nm thick) present at the crystal surface. Rapid growth rates would favor the entrapment of the enriched trace elements in the overgrowth region by increasing the diffusion distance. Accordingly, the partition coefficient of such elements increases with increasing calcite deposition rate. For elements with  $K_{Me} > 1$ , GEM predicts the depletion of trace metals in the near-surface region and thus inefficient diffusion due to a fast growth

rate, leading to growth exclusion and nonequilibrium partitioning. As a result, the partition coefficients of these elements decrease with increasing calcite deposition rate.

The partition coefficients of the cations  $Sr^{2+}$  and  $Ba^{2+}$  exhibit stronger correlations with the calcite growth rate than do those of other impurities in calcite, as demonstrated in Fig. 5. This result is consistent with the observed variations in trace element uptake with a growth rate under abiogenic conditions in the laboratory. Consequently, the concentrations of  $Sr^{2+}$  and  $Ba^{2+}$  in calcite are likely very sensitive indicators of calcite mineral growth, and the partitioning of  $Sr^{2+}$  and  $Ba^{2+}$  in natural calcite could be used as a potential tool for estimating the formation rate.

However, the partition coefficients of other metals with  $K_{Me} < 1$  do not show any correlation with deposition rate, indicating that the kinetic formation rate is not the main factor controlling the partitioning of these metal ions; other parameters would also play an important role. Moreover, the partition coefficients of all metals with  $K_{Me} > 1$  ( $Zn^{2+}$ ,  $Co^{2+}$ ,  $Mn^{2+}$ ,  $Cd^{2+}$ , etc) also display no correlation with the deposition rate, implying no influence of this factor on the partitioning of these metals between the two phases. Above all, these results suggest that the partitioning of most metal ions between solid and water phases in a natural travertine precipitation system would be controlled by multiple parameters other than a single factor. This finding should be taken into account when reconstructing the paleoenvironment or paleoclimate using trace element proxies in natural carbonate archives.

## 5 Conclusion

Metal partitioning between solid and solution in the natural travertine system showed a large variation in partition coefficients, with  $K_{Me} < 1$  for  $Li^+$ ,  $Na^+$ ,  $Mg^{2+}$ ,  $Sr^{2+}$  and  $Ba^{2+}$ ,  $K_{Me} > 1$  for  $Co^{2+}$ ,  $Mn^{2+}$ ,  $Zn^{2+}$  and  $Cu^{2+}$ , and a  $K_{Me}$  of approximately 1 for  $Ni^{2+}$ , consistent with previous laboratory experiments. The distributions of metals between the two phases were entirely consistent with the predicted behavior of the thermodynamic model, suggesting that the partitioning of metal ions into calcite under surface conditions was not, in general, an equilibrium process. Therefore, in addition to the inherent ionic characteristics of metals, such as the ionic radius and charge, external environmental parameters such as temperature, pH, and carbonate precipitation rate would also substantially affect metal distribution. Our results demonstrate that the partitioning of the metal cations  $Sr^{2+}$  and  $Ba^{2+}$  was mainly controlled by the calcite precipitation rate but the distributions of other metal ions were likely impacted by several, or even multiple, environmental parameters. As a result, one should pay attention to the specific

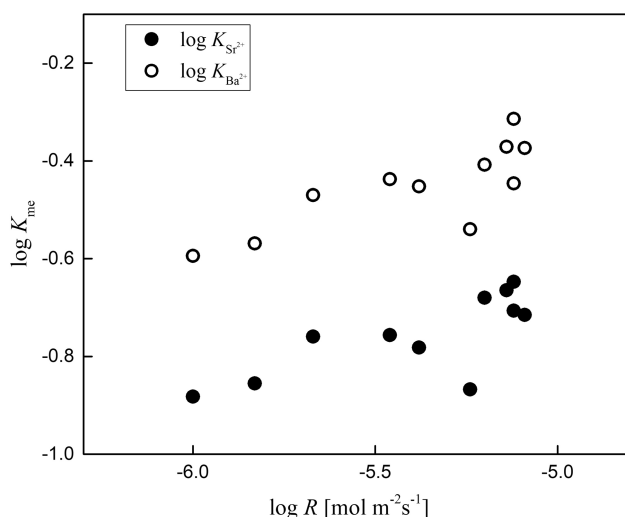


**Fig. 5**  $K_{me}$  of  $Mg^{2+}$  and  $Sr^{2+}$  as a function of calcite deposition rate

incorporation mechanism and the corresponding controlling factors when applying metal proxies in surface carbonate archives to reconstruct past environments. The results also imply that further systematic studies are needed to better constrain the trace metal distribution in both natural carbonate systems and laboratory experiments with regard to paleoenvironmental reconstruction. Such research work would also help reduce the uncertainty that arises in interpreting natural carbonate composition data and in paleoclimate reconstruction models employing the partitioning of elements as a proxy.

**Acknowledgements** This work was financially supported by the National Key Research and Development Program of China (2019YFC1804400), the National Natural Science Foundation of China (U1612442, 41961144028, 41625012, 41830647), “Ten Thousand Talent” project of Ministry of Science and Technology of the People’s Republic of China.

## References

- Burton EA, Walter LM (1991) The effects of  $P_{CO_2}$  and temperature on magnesium incorporation in calcite in seawater and  $MgCl_2$ – $CaCl_2$  solutions. *Geochim Cosmochim Acta* 55(3):777–785
- Carpenter SJ, Lohmann KC, Holden P et al (1991)  $\delta^{18}O$  values,  $^{87}Sr/^{86}Sr$  and  $Sr/Mg$  ratios of late devonian abiotic marine calcite: implications for the composition of ancient seawater. *Geochim Cosmochim Acta* 55(7):1991–2010
- Chen JB, Gaillardet J, Bouchez J et al (2015) Anthropophile elements in river sediments: overview from the Seine River. *Fr Geochem Geophys Geosyst* 15(11):4526–4546
- Crockett JH, Winchester JW (1966) Coprecipitation of zinc with calcium carbonate. *Geochim Cosmochim Acta* 30(10):1093–1109
- Curti E (1999) Coprecipitation of radionuclides with calcite: estimation of partition coefficients based on a review of laboratory investigations and geochemical data. *Appl Geochem* 14(4):433–445
- Doerner HA, Hoskins WM (1925) Co-precipitation of radium and barium sulfates. *J Am Chem Soc* 47(3):662–675
- Drake H, Mathurin FA, Zack T et al (2017) Incorporation of trace elements into calcite precipitated from deep anoxic groundwater in fractured granitoid rocks. *Procedia Earth Planet Sci* 17:841–844
- Dromgoole EL, Walter LM (1990) Iron and manganese incorporation into calcite: effects of growth kinetics, temperature and solution chemistry. *Chem Geol* 81(4):311–336
- Elzinga EJ, Rouff AA, Reeder RJ (2006) The long-term fate of  $Cu^{2+}$ ,  $Zn^{2+}$ , and  $Pb^{2+}$  adsorption complexes at the calcite surface: an X-ray absorption spectroscopy study. *Geochim Cosmochim Acta* 70(11):2715–2725
- Füger A, Konrad F, Leis A et al (2019) Effect of growth rate and pH on lithium incorporation in calcite. *Geochim Cosmochim Acta* 248:14–24
- Gaffey SJ (1987) Spectral reflectance of-carbonate minerals in the visible and near infrared (0.35–2.55 microns): calcite, aragonite, and dolomite. *J Geophys Res Atmos* 92(B2):1429–1440
- Gaillardet J, Dupré B, Louvat P et al (1999) Global silicate weathering and  $CO_2$  consumption rates deduced from the chemistry of large rivers. *Chem Geol* 159(1):3–30
- Gascoyne M (1983) Trace-element partition coefficients in the calcite-water system and their paleoclimatic significance in cave studies. *J Hydrol* 61(1):213–222
- Gaskova OL, Bukaty MB, Shironosova GP et al (2009) Thermodynamic model for sorption of bivalent heavy metals on calcite in natural-technogenic environments. *Russ Geol Geophys* 50(2):87–95
- Graham DW, Bender ML, Williams DF et al (1982) Strontium-calcium ratios in Cenozoic planktonic foraminifera. *Geochim Cosmochim Acta* 46(7):1281–1292
- Katz A (1973) The interaction of magnesium with calcite during crystal growth at 25–90 °C and one atmosphere. *Geochim Cosmochim Acta* 37(6):1563–1586
- Kinsman DJJ, Holland HD (1969) The co-precipitation of cations with  $CaCO_3$ —IV. The co-precipitation of  $Sr^{2+}$  with aragonite between 16 °C and 96 °C. *Geochim Cosmochim Acta* 33(1):1–17
- Kitano Y, Okumura M, Idogaki M (1980) Abnormal behaviors of copper (II) and zinc ions in parent solution at the early stage of calcite formation. *Geochim J* 14:167–175
- Lakshmanov LZ, Stipp SLS (2007) Experimental study of nickel (II) interaction with calcite: adsorption and coprecipitation. *Geochim Cosmochim Acta* 71(15):3686–3697
- Liu C, Wang Z, Raub TD (2013) Geochemical constraints on the origin of marinoan cap dolostones from nuccaleena formation, South Australia. *Chem Geol* 351:95–104
- Liu SL, Wang ZW, Zhang YY et al (2019) Distribution and partitioning of heavy metals in large anthropogenically impacted river, the Pearl River. *China Acta Geochim* 38(2):216–231
- Liu Z, Li H, You C et al (2006) Thickness and stable isotopic characteristics of modern seasonal climate-controlled sub-annual travertine laminas in a travertine-depositing stream at Baishuitai, SW China: implications for paleoclimate reconstruction. *Environ Geol* 51(2):257–265
- Liu Z, Zhang M, Li Q et al (2003) Hydrochemical and isotope characteristics of spring water and travertine in the Baishuitai area (SW China) and their meaning for paleoenvironmental reconstruction. *Environ Geol* 44(6):698–704
- Lorens RB (1981) Sr, Cd, Mn and Co distribution coefficients in calcite as a function of calcite precipitation rate. *Geochim Cosmochim Acta* 45(4):553–561
- Luo W, Wang S, Xie X et al (2013) Temporal and spatial variations in hydro-geochemistry of cave percolation water and their implications for four caves in Guizhou. *China Chin J f Geochem* 32(2):119–129
- Mavromatis V, Gautier Q, Bosc O et al (2013) Kinetics of Mg partition and Mg stable isotope fractionation during its incorporation in calcite. *Geochim Cosmochim Acta* 114:188–203
- Morse JW, Bender ML (1990) Partition coefficients in calcite: examination of factors influencing the validity of experimental results and their application to natural systems. *Chem Geol* 82:265–277
- Mucci A (1987) Influence of temperature on composition of magnesian calcite overgrowth precipitated from seawater. *Geochim Cosmochim Acta* 51:1977–1984
- Mucci A, Morse JW (1983) The incorporation of  $Mg^{2+}$  and  $Sr^{2+}$  into calcite overgrowths: influences of growth rate and solution composition. *Geochim Cosmochim Acta* 47(2):217–233
- Okumura M, Kitano Y (1986) Coprecipitation of alkali metal ions with calcium carbonate. *Geochim Cosmochim Acta* 50(1):49–58
- Pingitore NE, Eastman MP (1984) The experimental partitioning of  $Ba^{2+}$  into calcite. *Chem Geol* 45(1):113–120
- Pingitore NE, Eastman MP (1986) The coprecipitation of  $Sr^{2+}$  with calcite at 25 °C and 1 atm. *Geochim Cosmochim Acta* 50(10):2195–2203

- Reeder RJ, Lamble MG, Northrup P (1999) XAFS study of the coordination and local relaxation around  $\text{Co}^{2+}$ ,  $\text{Zn}^{2+}$ ,  $\text{Pb}^{2+}$ , and  $\text{Ba}^{2+}$  trace elements in calcite. *Am Mineral* 84:1049–1060
- Rimstidt JD, Balog A, Webb J (1998) Distribution of trace elements between carbonate minerals and aqueous solutions. *Geochim Cosmochim Acta* 62(11):1851–1863
- Roberts MS, Smart PL, Baker A (1998) Annual trace element variations in a Holocene speleothem. *Earth Planet Sci Lett* 154(1):237–246
- Roberts N, Wright JHE (1993) Vegetational, lake-level, and climatic history of the near east and southwest Asia. *Glob Clim Since Last Glacial Maximum* 194–220
- Rosenthal Y, Boyle EA, Slowey N (1997) Temperature control on the incorporation of magnesium, strontium, fluorine, and cadmium into benthic foraminiferal shells from Little Bahama Bank: prospects for thermocline paleoceanography. *Geochim Cosmochim Acta* 61(17):3633–3643
- Schott J, Mavromatis V, González-González A et al (2014) Kinetic and thermodynamic controls of divalent metals isotope composition in carbonate: experimental investigations and applications. *Procedia Earth and Planet Sci* 10:168–172
- Sverjensky DA (1984) Prediction of gibbs free energies of calcite-type carbonates and the equilibrium distribution of trace elements between carbonates and aqueous solutions. *Geochim Cosmochim Acta* 48(5):1127–1134
- Tesoriero AJ, Pankow JF (1996) Solid solution partitioning of  $\text{Sr}^{2+}$ ,  $\text{Ba}^{2+}$ , and  $\text{Cd}^{2+}$  to calcite. *Geochim Cosmochim Acta* 60(6):1053–1063
- Tsue A, Holland HD (1966) The coprecipitation of cations with  $\text{CaCO}_3$ -III. The coprecipitation of  $\text{Zn}^{2+}$  with calcite between 50 °C and 250 °C. *Geochim Cosmochim Acta* 30:439–453
- Watson EB (1996) Surface enrichment and trace-element uptake during crystal growth. *Geochim Cosmochim Acta* 60(24):5013–5020
- Watson EB (2004) A conceptual model for near-surface kinetic controls on the trace-element and stable isotope composition of abiogenic calcite crystals. *Geochim Cosmochim Acta* 68(7):1473–1488
- White AF (1977) Sodium and potassium coprecipitation in aragonite. *Geochim Cosmochim Acta* 41(5):613–625
- White WM (2011) Trace elements in igneous processes. *Geochemistry* 265–317
- Yan H, Schmitt A, Liu Z et al (2016) Calcium isotopic fractionation during travertine deposition under different hydrodynamic conditions: examples from Baishuitai (Yunnan, SW China). *Chem Geol* 426:60–70
- Zhong S, Mucci A (1995) Partitioning of rare earth elements (REEs) between calcite and seawater solutions at 25 °C and 1 atm, and high dissolved REE concentrations. *Geochim Cosmochim Acta* 59(3):443–453